Lattice distortions and short-range magnetic order in classical magnetoelastic Heisenberg chains

M. Marchand, A. Caillé, and R. Pépin
Département de Physique et Centre de Recherche en Physique du Solide, Université de Sherbrooke, Sherbrooke, Québec J1K 2R1, Canada
(Received 7 April 1986)

Lattice distortions of a two-dimensional array of one-dimensional classical Heisenberg spin chains with magnetoelastic coupling are studied in the limit of strong interchain elastic interactions. Exact integration over the spin degrees of freedom leads to a temperature-dependent free-energy functional of the elastic variables only. The equilibrium lattice structure is obtained from the ground state of this free-energy functional and the phase diagram indicates the presence of a tricritical point. The necessity of performing the calculations at constant pressure is stressed and it is shown that a dimerized phase could be reached by applying pressure to certain magnetic materials, provided that there exist positive second-neighbor elastic interactions. The consequences of lattice distortions on the short-range magnetic order are studied by calculating the wave-number-dependent magnetic susceptibility. It is found that the dominant short-range magnetic order is of period four in the dimerized lattice phase.

I. INTRODUCTION

Magnetoelasticity and magnetostriction have been the subject of much theoretical and experimental research for more than 30 years. One long-standing controversy concerns the order of the magnetic transition in the presence of a magnetoelastic coupling. In order to obtain a reliable answer to this problem, renormalization-group calculations have been performed by Sak,[1] Bergman and Halperin,[2] de Moura *et al.*,[3] and many others.[4] By the Wikson-Kadanoff momentum shell integration technique on an elastic continuum Hamiltonian, it has been found by ϵ expansion that the order of the transition depends mostly on the constraints (constant volume or constant pressure), the rotational symmetry of the elastic continuum, and the boundary conditions. Unfortunately, this kind of continuum approach, although quite successful for handling the $q=0$ instabilities, is not suited to deal with instabilities near the zone boundaries. In this paper we shall study a simple microscopic model in which such instabilities are produced by a magnetoelastic coupling; we show that these may induce new magnetic short-range order at finite temperature T and possibly new magnetic phases at $T=0$.

The model consists of one-dimensional (1D) classical Heisenberg spin chains interacting with three-dimensional (3D) elastic variables. It will be shown that, even if the 1D interacting spin system cannot sustain long-range magnetic order at finite T, it can create, by means of a magnetoelastic coupling, nonuniform lattice instabilities and thus a phase transition at finite T for elastic variables interacting in three dimensions. This lattice distortion will in turn affect the short-range magnetic order and thus its long-range order at $T=0$ in the distorted lattice phase. In particular, it will be shown that the dominant short-range magnetic order in a dimerized phase is of period 4 (the spin configuration: $\uparrow\uparrow\downarrow\downarrow\uparrow\uparrow\ldots$). In this way, the magnetoelastic coupling changes the form of the long-range and short-range order present in the bare lattice and the bare 1D magnetic system.

The analogue of this model for Ising chains has been treated by Pytte.[5] Our approach differs greatly from his since we cannot convert our classical Heisenberg model to a pseudo spin problem. Nevertheless, our results are quite similar to his. However, in addition, we show that a dimerized phase could be reached by applying pressure in certain magnetic materials, provided that there exist positive second-neighbor elastic interactions. It will become clear that there cannot be any nonuniform lattice distortion in a translationally invariant 1D spin system on a 3D lattice with only first-neighbor interactions present, since the lattice free energy is then simply a sum of bond-free energies. In addition to this, we shall investigate the short-range magnetic order in the presence of a lattice distortion by a calculation of the wave-number-dependent magnetic susceptibility.

This problem has been treated previously by Penson *et al.*[6,7] for an incompressible chain. Our results show that such an approach is not justified for magnetoelastic problems since the integration over the spin variables yields, in general, an equivalent pressure term. Therefore, for experimental applicability, calculations should be performed at constant pressure. Nevertheless, we recover their results in the limit of very large second-neighbor elastic interactions compared to the first-neighbor elastic interactions since the chains are then incompressible. Our approach also differs in that we did not make a Landau expansion of the bond-free energy $W(x)$, as did Penson *et al.*,[6,7] noting that each term Δ^n of such an expansion is multiplied by $(J_1/k_BT)^n$, where J_1 is the first derivative of the exchange integral evaluated at the equilibrium bond length. It is easily verified that such an expansion is ha-

zardous since we are interested in the limit $k_BT \ll J_1$. In fact, it is mathematically easier, and of course more rigorous, to work with the exact form of $W(x)$.

The organization of this paper is as follows. By an exact integration in spin space we derive, in Sec. II, a free-energy functional of the elastic variables only. The equilibrium lattice structure will be obtained from the stationary configuration corresponding to the lowest minimum of this free-energy functional, which we refer to as the ground state. In Sec. III we show that since the ground state is either uniform or dimerized, we only need two variables to find them. In Sec. IV we present the phase diagram for the lattice structure and show how the dimerized phase can be reached at low temperatures for some magnetic materials by means of a positive applied pressure. In Sec. V we investigate the kind of short-range magnetic order present upon lattice distortion, by calculating the wave-number-dependent magnetic susceptibility. Finally, the main results are discussed and summarized in Sec. VI.

II. EXACT FREE-ENERGY FUNCTIONAL OF ELASTIC VARIABLES

In order to study the form of the lattice distortion that occurs in a two-dimensional array of classical Heisenberg spin chains coupled together by means of elastic interactions, it is important to avoid unnecessary complications. Thus we assume that all the elastic interchain couplings are identical and sufficiently strong to achieve a 3D structural long-range order with all the elastic variables in phase with their interchain nearest neighbors. In this case the identical distortion (if any) of each chain can only be modulated along one direction and all the transverse elastic couplings need not be included in the Hamiltonian. This kind of elastic anisotropy can be found in certain quasi-one-dimensional magnetic systems[8] that have a high-temperature structural rearrangement which prepares the softening of the lattice in one particular direction without softening in the other two directions. Therefore, as a model for this physical problem, we propose the following one-dimensional translationally invariant Hamiltonian H for N atoms:

$$H=K_1\sum_{j=1}^{N-1}(u_{j+1}-u_j-a_1)^2+p\sum_{j=1}^{N-1}(u_{j+1}-u_j)+K_2\sum_{j=1}^{N-2}(u_{j+2}-u_j-2a_2)^2+\sum_{j=1}^{N-1}J(u_{j+1}-u_j)\mathbf{S}_j\cdot\mathbf{S}_{j+1}\,, \tag{2.1}$$

where the u_j's describe the absolute locations of the atoms along the chains under the external pressure (or tension) p. The equilibrium distance a_1 of positive first-neighbor elastic interactions (K_1) could, in general, be different from the half-equilibrium distance a_2 of the positive second-neighbor term K_2. These atoms also possess classical spin degrees of freedom which are described by a 3D Heisenberg unit vector $\mathbf{S}_j$ interacting with first neighbors through the exchange integral J, which is a function of the atom's spacing.

$J(u_{j+1}-u_j)$ is expanded around the first-neighbor equilibrium distance a_1 and only the linear part is kept:

$$J(u_{j+1}-u_j)=J(a_1)+(u_{j+1}-u_j-a_1)J'(a_1) \tag{2.2}$$

where $J'(a_1)$ is the first derivative of $J(x)$ evaluated at $x=a_1$. Making use of the simple gauge transformation,

$$u_j=ja_1+x_j\,, \tag{2.3}$$

and rewriting (2.1) in terms of x_j with the linear approximation (2.2), we obtain[9] (apart from a constant independent of the degrees of freedom)

$$H=K_1\sum_{j=1}^{N-1}(x_{j+1}-x_j)^2+P\sum_{j=1}^{N-1}(x_{j+1}-x_j)+K_2\sum_{j=1}^{N-2}(x_{j+2}-x_j)^2+\sum_{j=1}^{N-1}[J_0-(x_{j+1}-x_j)J_1]\mathbf{S}_j\cdot\mathbf{S}_{j+1}\,, \tag{2.4}$$

where $J_0=J(a_1)$, $J_1=-J'(a_1)$, and $P=p-8K_2(a_2-a_1)$. Note that the misfit (a_2-a_1) of the elastic interactions simply renormalizes the pressure term. However, if the magnetoelastic coefficient J_1 is zero, the spins decouple totally from the elastic variables, and the harmonic lattice, described by the first three terms on the right-hand side of (2.4), has a uniform stable ground state[10] given by

$$v_j=x_{j+1}-x_j=-P/(2K_1+8K_2)\,.$$

Therefore there is no "built-in" instability in the bare lattice.

Now the central question we want to answer is the following: Is there any 3D structural order that can bifurcate from the uniform state when the harmonic lattice is coupled through J_1 to the 1D Heisenberg chains? It is informative to begin with a qualitative analysis of the effect of the magnetoelastic coupling in order to understand the physical origin of the effective lattice Hamiltonian obtained below from an exact integration over the classical spin degrees of freedom. Let us first define a bond-dependent exchange integral, $y_j=J_0-J_1v_j$, where $v_j=x_{j+1}-x_j$ is the bond variable. From the Hamiltonian (2.4) it can be seen that an increase in the absolute value of y_j always leads to a decrease in the energy of the magnetic term, regardless of the sign of the exchange integral. In the presence of magnetoelastic coupling, y_j changes as a result of variations in the bond length. For small lattice distortions, the dominant term is given by (2.2) and hence the gain in magnetic energy depends linearly on the distortion. This linear dependence, combined with the quadratic dependence of the elastic energy, gives rise to a new equilibrium bond length. If the exchange integrals y_j can pass through zero, as in Fig. 6, then there can be two equilibrium positions for each bond. Therefore, the total energy of each bond will have the form of a double-well potential and the net result is an "overscreening" of the first-neighbor elastic interaction K_1 by the magnetoelastic coupling. At finite temperature, this effect will be smeared by 1D spin fluctuations and thus we expect that the effective double-well bond energy will appear at a cer-

tain critical temperature. However, if only first-nearest-neighbor interactions were present, then the 3D lattice structure would be driven, by J_1, towards a uniformly distorted array of linear chains. This explains the importance of the second-nearest-neighbor elastic interaction K_2. By restricting the variation in the second-nearest-neighbor equilibrium distance, K_2 forces successive bond lengths to alternate. Let us now return to a quantitative analysis of this phenomena.

The 3D equilibrium lattice structure will then be the ground state of the following (temperature-dependent) energy functional F_e of the elastic variables obtained by integrating over the classical spin degrees of freedom,

$$\exp(-\beta F_e)=\int \frac{d\Omega_1}{4\pi}\cdots\frac{d\Omega_N}{4\pi}\exp(-\beta H)\ , \tag{2.5}$$

where $\beta=1/k_BT$, $d\Omega_j=\sin(\theta_j)d\theta_j d\phi_j$, and (θ_j,ϕ_j) are the spherical polar angles of the unit vector $\mathbf{S}_j$. Fortunately, (2.5) can be evaluated exactly because of the unidimensionality of the spin interactions, the absence of an external magnetic field, and the isotropy of the exchange integrals. To perform these integrations, one expresses $\mathbf{S}_j$ with respect to $\mathbf{S}_{j+1}$ during the integration over $d\Omega_j$ (starting with $\mathbf{S}_1$). We immediately find (apart from a constant, independent of T, and of the elastic variables),

$$F_e=\sum_{j=1}^{N-1}W(y_j)+B\sum_{j=1}^{N-1}y_j+C\sum_{j=1}^{N-2}(y_{j+1}+y_j)^2\ , \tag{2.6}$$

where

$$W(y)=2^{-1}y^2-\beta^{-1}\ln[\sinh(\beta y)/(\beta y)]\ , \tag{2.7}$$

$$B=-(P/J_1)-2J_0(K_1+4K_2)/J_1^2\ , \tag{2.8}$$

and

$$C=K_2/2K_1\ . \tag{2.9}$$

All the energy quantities like y_j are scaled by $J_1^2/2K_1$. $W(y)$ is plotted in Fig. 1 for different temperatures $\tau=1/\beta$. It is clear that $W(y)$ becomes a double-well potential for $\tau<\frac{1}{3}$. At $t=0$ it is described by the double quadratic well

$$W(y)\,|_{T=0}=\{[y-\mathrm{sgn}(y)]^2-1\}/2\ , \tag{2.10}$$

where $\mathrm{sgn}(y)=+1$ for $y>0$ and -1 for $y<0$.

Therefore the effects of the 1D spin system on the elastic variables is twofold. Firstly, the first-neighbor elastic interaction K_1 is "overscreened," so that if $B=0$, the uniform ground state of (2.6) bifurcates into a dimerized ground state at $\tau=\frac{1}{3}$ for $C>0$. Secondly, the pressure term is renormalized for a nonzero value of J_0 giving the linear ($y\leftrightarrow -y$) symmetry-breaking term B. Since magnetic materials have in general a nonzero value of J_0, it is essential for physical realism to study the effects of the B term. Furthermore, it is an experimentally accessible parameter that can be changed by varying the pressure p. However, it is to be noticed that the symmetry-breaking field B only affects the $q=0$ part of the free energy F_e. This means that it cannot create, by itself, an instability of periodicity other than the one included in the remaining part of F_e [in our case, $W(y)$ and C]. Nevertheless, it changes the $y_{q=0}$ part of the ground state, and hence modifies the transition temperature. In fact, B can suppress the transition completely if it is large enough.

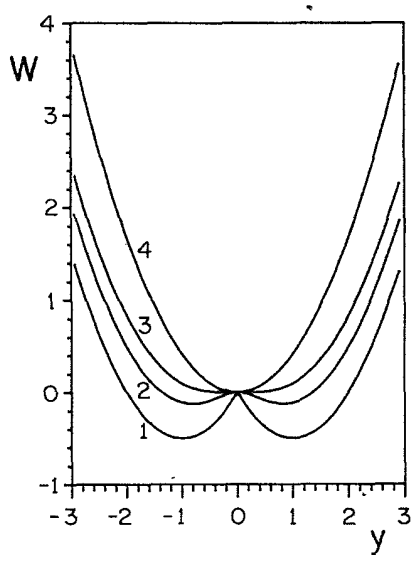

FIG. 1. The function $W(y)$ for various values of the temperature. Curves 1, 2, 3, and 4 are for $\tau=0.0$, 0.15, 0.3333, and 2.0, respectively.

It is important to realize that it is the overscreening effect of the magnetoelastic coupling on K_1 that produces the lattice instability and that a dimerization can occur only in the presence of a positive K_2. But it should be mentioned once again that there is no instability in the bare lattice even in the presence of K_2. The instability occurs because of the linear magnetoelastic coupling J_1. In the following sections we will find the 3D equilibrium lattice structures, given by the ground state of F_e, for various values of B, C, and τ. This description, which is essentially of the mean-field type, neglects fluctuations out of these ground states and the results so obtained should be realistic outside the critical region.

III. REDUCTION TO TWO DEGREES OF FREEDOM

For $B=0$, the ground state of F_e is easily found. It is the uniform state $y_j=0$ for $\tau>\frac{1}{3}$ and it bifurcates to a double degenerate dimerized state for $\tau<\frac{1}{3}$ and $C>0$. Therefore, in this translationally invariant model, the positive second-neighbor elastic term is essential to stabilize the dimerized state. Without any next-nearest-neighbor interactions, F_e is reduced to a sum of bond-free energies and the ground state is either a uniform state if W has a single nondegenerate minimum (i.e., for $\tau>\frac{1}{3}$ or $\tau<\frac{1}{3}$ and $B\neq 0$) or a random deformed state which is $2(N-1)$-fold degenerate if W has 2 degenerate minima (i.e., for $\tau<\frac{1}{3}$ and $B=0$). This result is to be contrasted with the behavior predicted for the quantum spin-Peierls transition[8,11] where dimerization results from $2k_F$ nesting of the quasifermions and is present even in the absence of the second-neighbor elastic term.

For nonzero value of B, the ground state is modified by a uniform distortion and the dimerized instability will manifest itself at $\tau<\frac{1}{3}$. As already mentioned, the B term cannot produce an instability of different periodicity than the one involved in W and C. Therefore the ground state of F_e is always either uniform or dimerized. Then, without loss of generality, we only need two independent variables y_1 and y_2, the two exchange integral value of adjacent bonds, to describe the equilibrium lattice structure $\{y_j\}=(y_1,y_2,y_1,y_2,\ldots)$. It is double degenerate if y_1 is different than y_2 (in the dimerized state). Therefore, the ground state of the free energy may be found by minimizing $f_e=F_e/(N-1)$ which reads

$$f_e=2^{-1}[f_u(y_1)+f_u(y_2)]-C(y_1-y_2)^2 , \tag{3.1}$$

where $f_u(y)$, the free energy per bond in the uniform state $y_1=y_2=y$, is given by

$$f_u(y)=W(y)+By+4Cy^2 . \tag{3.2}$$

The extremum conditions[12] $\partial_{y_1}f_e=0$ and $\partial_{y_2}f_e=0$ give

$$y_1-y_2=L(\beta y_1)-L(\beta y_2) , \tag{3.3a}$$

$$y_1+y_2=A[L(\beta y_1)+L(\beta y_2)]+2g , \tag{3.3b}$$

where $A=(1+8C)^{-1}$, $g=-AB$, and $L(x)=\coth(x)-1/x$ is the Langevin function. Since $K_2\geq 0$ and $K_1>0$, A is constrained to the interval [0,1]. In the uniform state, (3.3) reduces to

$$y=AL(\beta y)+g . \tag{3.4}$$

Since f_e is a function of only two independent variables, stability of the extrema of f_e is assured by requiring[13] that

$$\begin{vmatrix} \partial^2_{y_1^2}f_e & \partial_{y_1}\partial_{y_2}f_e \\ \partial_{y_1}\partial_{y_2}f_e & \partial^2_{y_2^2}f_e \end{vmatrix}>0 \tag{3.5a}$$

and

$$\partial^2_{y_1^2}f_e>0 , \tag{3.5b}$$

where all the derivatives are evaluated at the solutions (y_1,y_2) of (3.3). Consequently, a solution of (3.3) is a local minimum of f_e only if

$$\tau^2+AL'(\beta y_1)L'(\beta y_2)-\tau(1+A)[L'(\beta y_1)+L'(\beta y_2)]/2>0 \tag{3.6a}$$

and

$$L'(\beta y_1)<\tau(1+A^{-1})/2 , \tag{3.6b}$$

where $L'(x)$ is the first derivative of $L(x)$. For the uniform state $y_1=y_2=y$, the stability conditions (3.5) reduce to $\partial^2_{y^2}f_u>0$. Using (3.2), this can be written as

$$\tau>AL'(\beta y) . \tag{3.7}$$

In summary, for a given set of (τ,g,A), the ground state is the configuration of lowest energy f_e amongst the uniform states [satisfying (3.4) under the stability constraint (3.7)] or the dimerized states [satisfying (3.3) under the constraints (3.6)].

IV. PHASE DIAGRAM FOR THE LATTICE STRUCTURE

At $T=0$, Eqs. (3.3) and (3.4), subject to the constraints (3.6) and (3.7) are easily solved to obtain the phase diagram in Fig. 2. Since $W(y)$ has two minima, two uniform states are obtained: $y_1=y_2=y^+=A+g$, which is stable for $g>-A$, and $y_1=y_2=y^-=-A+g$, which is stable for $g<A$. A doubly degenerate dimerized state $(y_1,y_2)=(g+1,g-1)$ is stable for $-1<g<1$ and is the absolute ground state for $(A-1)/2<g<(1-A)/2$. Because of large metastable regions in parameter space, all transitions would be accompanied by hysteresis effects around the first-order transitions at $g=\pm(1-A)/2$ where the uniform state bifurcates discontinuously to an alternating (i.e., single-bond ferromagnetic and the other antiferromagnetic) dimerized state. The dependence of the phase diagram on the ratio of next-nearest- to nearest-neighbor elastic interactions is obtained by varying A. For example, if $A=1$ ($C=0$) the ground state is always uniform but there is a discontinuous change of chain length (first-order transition) at $g=0$.

At finite temperature T Eqs. (3.3), (3.4), (3.6), and (3.8) are solved numerically. A typical phase diagram for the value $A=\frac{1}{2}$ is presented in Fig. 3. A tricritical point separating the regions of first- and second-order transitions is obtained. At $T=0$, the results of Fig. 2 are recovered. In Appendix A, the calculation of the exact position of the tricritical point as function of A is presented. The results are plotted in Fig. 4. For $A=0$ (C infinite), we obtain $\tau_T=0.237\,38(6)$, in agreement with the result of Penson *et al.*[6,7] for the incompressible chain. Phase diagrams for different values of A are plotted in Fig. 5. The tricritical points were obtained using Appendix A. The dimerized region collapses on the $g=0$ line as A goes to 1, indicating the absence of a dimerized state for $K_2=0$. Since the phase diagrams are symmetric with respect to an inversion of g, only the parts $g>0$ are shown. On the other hand, the solutions (y_1,y_2) become $(-y_2,-y_1)$ upon an inversion of g and $(y,-y)$ at $g=0$ (for $C>0$).

The dominant feature of Fig. 5 is that the dimerized

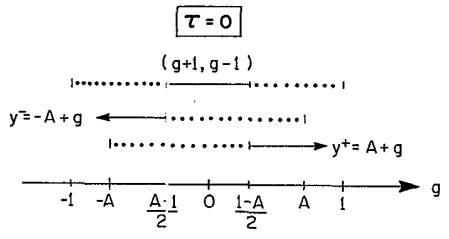

FIG. 2. The $T=0$ phase diagram and stability regions for the two uniform phases (y^+ and y^-) and the dimerized (doubly degenerate) state $(y_1,y_2)=(g+1,g-1)$. The dotted lines indicate metastable states and the solid lines the ground states.

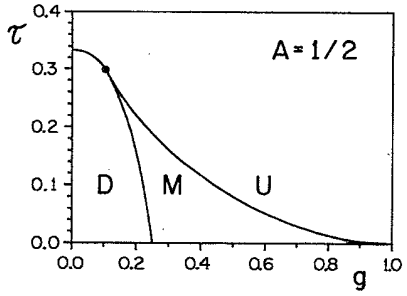

FIG. 3. Phase diagram and stability regions for $A=\frac{1}{2}$. The ground state is a dimerized state in region D and a uniform state in regions M and U. The dimerized state is metastable in region M. The large dot represents a tricritical point above which the transition is second order and below which it is first order.

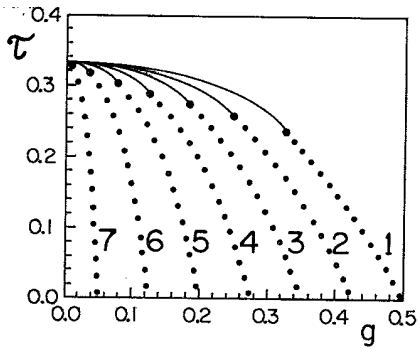

FIG. 5. The phase diagram for different values of A: $A=0.0$, 0.15, 0.30, 0.45, 0.60, 0.75, and 0.90, for curves 1, 2, 3, 4, 5, 6, and 7, respectively. The dotted lines are first-order transitions and the solid lines are second-order ones. The dimerized state is the ground state in the region below the curve for a given A. The large dots are tricritical points.

phase is possible only for $\tau<\frac{1}{3}$ and $|g|$ smaller than a value which is a function of A: $|g|<(1-A)/2$ for $T=0$. The pressure needed to be in the dimerized region depends on the type of magnetic material. Four different types of magnetoelastic materials with nonzero value of J_1 are located on a typical curve (see Fig. 6) of the exchange integral versus first-neighbor distance. Recall that J_0 and J_1 are, respectively, the value of the exchange integral and negative value of the gradient evaluated at a_1. Since $g=J_0+AP/J_1$, a positive applied pressure could drive materials of type 2 and 4 of Fig. 6 into the dimerized phase by lowering the absolute value of g. The order of magnitude of the pressure needed depends on J_0, J_1, and A. A rough estimate[14] indicates that it is quite accessible for a system that would have a presoftening mechanism (small K_1) at a higher temperature. Materials of type 1 and 3 are driven further away from the dimerized region by a positive applied pressure since the value of $|g|$ then increases. By the inverse argument, if a negative applied pressure (stretching the crystal) could be realized experimentally, it would drive materials of type 1 and 3 into the dimerized phase and materials of type 2 and 4 away from it.

Figures 7(a), 8(a), and 9(a) illustrate the typical behavior of the exchange integrals y as a function of g for $\tau>\tau_T$, $\tau=\tau_T$, and $\tau<\tau_T$. These results are numerical solutions of (3.3), (3.4), (3.6), and (3.7). Again, only the part $g>0$ is shown [recall that (y_1,y_2) becomes $(-y_2,-y_1)$ upon changing g into $-g$]. For $g>0$, the uniform state has an antiferromagnetic exchange integral whereas it has a ferromagnetic exchange integral for $g<0$. This uniform state bifurcates into the dimerized state at some critical value of g (given in Fig. 5), continuously for $\tau>\tau_T$ and discontinuously for $\tau<\tau_T$ to two values of y in the dimerized state. Numerically, a continuous increase in the jump of y_1-y_2 starting at zero for $\tau=\tau_T$ and going to 2 at $\tau=0$ is observed. These figures represent either dilation of contraction (relative to a_1) of the bonds, depending on the sign of J_1 for a given material. For example, if $J_1>0$, an increase of y represents a decrease in bond length whereas it is an increase for $J_1<0$. Note also that since J_1 enters in g, an increase of g represents an increase of p for $J_1>0$ but a decrease of p for $J_1<0$.

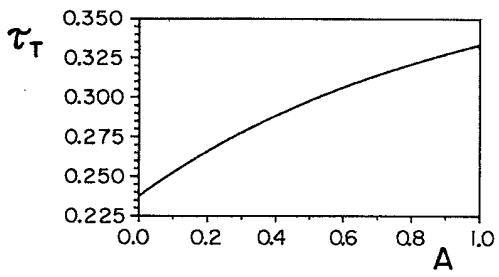

FIG. 4. Temperature τ_T of the tricritical point as a function of A.

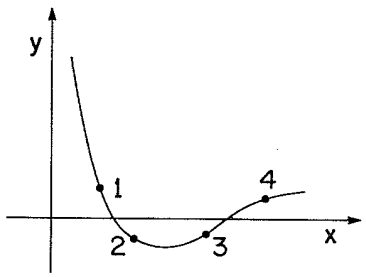

FIG. 6. Schematic representation of the exchange integral y as a function of the nearest-neighbor distance x. The dots represent the actual value of y at the first-neighbor elastic interaction equilibrium distance a_1 for four different types of magnetic materials. We have $J_0>0$ and $J_1>0$ for material 1, $J_0<0$ and $J_1>0$ for material 2, $J_0<0$ and $J_1<0$ for material 3, and finally, $J_0>0$ and $J_1<0$ for material 4.

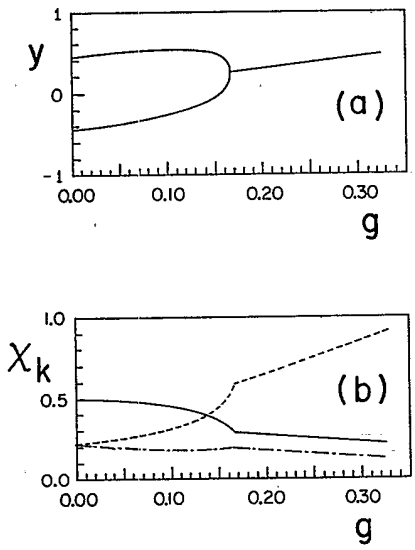

FIG. 7. (a) Bifurcation of the exchange integral y of the uniform state to two values (represented by the upper branch and the lower branch) in the dimerized state. $A=0.3$ and $\tau=0.29>\tau_T$. (b) Calculations of χ_k from the solution (a). The solid line is for $k=\pi/2$, the dashed line for $k=\pi$, and the dotted-dashed line for $k=0$.

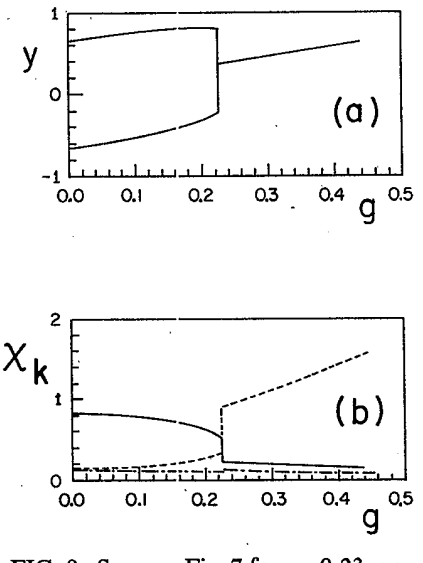

FIG. 9. Same as Fig. 7 for $\tau=0.23<\tau_T$.

V. SHORT-RANGE MAGNETIC ORDER

A 1D spin system cannot sustain any long-range magnetic order. Nevertheless, we have shown that it can induce a lattice instability in a 3D elastic crystal as a result of magnetoelastic coupling. One convenient way to see how this lattice instability in turn affects the short-range magnetic order is by a study of the wave-number-dependent magnetic susceptibility χ_k. The value of k for which χ_k has the largest value gives the dominant short-range magnetic order period $2\pi/k$ present in the spin system. For example, if the maximum value of χ_k is at $k=0$ ($k=\pi$) the dominant short-range magnetic order is ferromagnetic (antiferromagnetic). If it is at $k=\pi/2$, the dominant short-range order is of period 4 (the spin configuration: $\uparrow\uparrow\downarrow\downarrow\uparrow\uparrow\downarrow\downarrow\cdots$).

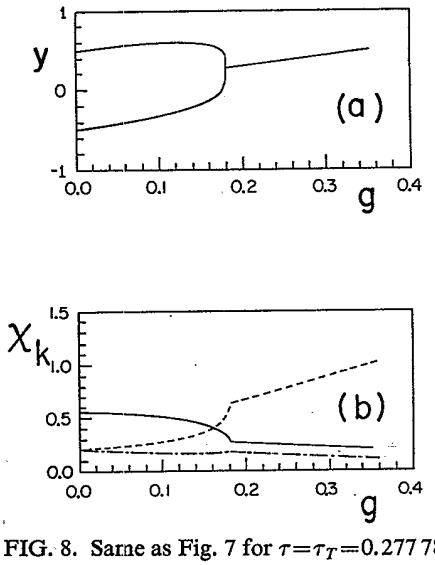

FIG. 8. Same as Fig. 7 for $\tau=\tau_T=0.277\,78$.

The wave-number-dependent static magnetic susceptibility χ_k is defined as the linear response of $\langle S_k^z\rangle$;

$$\chi_k=(\partial_{h_k}\langle S_k^z\rangle)_{h_k=0} \tag{5.1}$$

to a small external magnetic field (whose direction defines the z axis). The additional contribution H_{ext} to the Hamiltonian is

$$H_{\text{ext}}=-\sum_{j=1}^{N}h_jS_j^z=-\sum_{k=-\pi}^{+\pi}h_kS_{-k}^z\,, \tag{5.2}$$

here we have used the Fourier series,

$$h_j=N^{-1/2}\sum_{k=-\pi}^{+\pi}h_ke^{ikj}\,, \tag{5.3a}$$

$$S_j^z=N^{-1/2}\sum_{k=-\pi}^{+\pi}S_k^ze^{ikj}\,. \tag{5.3b}$$

Therefore, (5.1) gives the usual correlation function:

$$\chi_k=\beta\langle S_k^zS_{-k}^z\rangle$$
$$=(\beta/N)\sum_{l,m=1}^{N}e^{-ik(l-m)}\langle S_1^zS_m^z\rangle\,, \tag{5.4}$$

where now $\langle\ \rangle$ stands for the thermal average without H_{ext}. It is shown in Appendix B that, for an arbitrary configuration of exchange integrals $\{y_j\}$, we have

$$\langle S_j^zS_{j+n}^z\rangle=3^{-1}\prod_{l=j}^{j+n-1}L(-\beta y_l) \tag{5.5}$$

for $n>1$ [$\langle(S_j^z)^2\rangle=\frac{1}{3}$]; and $L(x)$ is the Langevin function. Inserting (5.5) into (5.4) and making extensive use of finite geometrical progressions, we obtain for a dimerized chain $\{y_j\}=(y_1,y_2,y_1,y_2\cdots)$ of N spins:

$$\langle S_k^z S_{-k}^z \rangle = \frac{1}{3N}\left[N + \frac{x^2}{1-x^2}\left[(N-2) + \frac{(1+x^2)x^{N-1} - 2x^2}{1-x^2}\right] + \text{c.c.} + \frac{L_1+L_2}{(L_1L_2)^{1/2}}\frac{x}{1-x^2}\left[\frac{N-1}{2} + \frac{x^{N+1}-x^2}{1-x^2}\right] + \text{c.c.}\right], \tag{5.6}$$

where

$$x = (L_1L_2)^{1/2}e^{ik}. \tag{5.7}$$

$L_1 = L(-\beta y_1)$, $L_2 = L(-\beta y_2)$, and c.c stands for the complex conjugate of the preceding term. We recover the result of Fisher[15] for the uniform chain if $L_1 = L_2$. In the thermodynamic limit of N going to infinity, (5.6) reduces to

$$\langle S_k^z S_{-k}^z \rangle = 3^{-1}\left[\frac{(1-L_1L_2)[(1+L_1L_2)+(L_1+L_2)\cos(k)]}{(1-L_1L_2)^2 + 4L_1L_2\sin^2(k)}\right]. \tag{5.8}$$

In order to investigate the kind of singularity that occurs in χ_k at $T=0$, we use the following asymptotic expansion:

$$L(|x| \gg 1) = \pm 1 - x^{-1} + O(e^{\mp 2x}). \tag{5.9}$$

the $T=0$ limit of χ_k for the uniform chain becomes

$$\lim_{T\to 0+} \chi_k = \mp(3y)^{-1}\left[\frac{[1 \pm (\beta y)^{-1} + (\beta y)^{-2}] + [(\beta y)^{-1} \pm 1]\cos(k)}{(\beta y)^{-2} + \sin^2(k)}\right], \tag{5.10}$$

where the upper (lower) sign stands for the ferromagnetic (antiferromagnetic) case. The only singularities in (5.10) are for $k=0$ and $k=\pi$. For the antiferromagnetic ($y>0$) case, we have

$$\lim_{T\to 0+} \chi_{k=0} = (6y)^{-1}, \tag{5.11a}$$

$$\lim_{T\to 0+} \chi_{k=\pi} = \tfrac{2}{3}\beta^2 y, \tag{5.11b}$$

and for the ferromagnetic ($y<0$) case we have

$$\lim_{T\to 0+} \chi_{k=0} = -\tfrac{2}{3}\beta^2 y, \tag{5.12a}$$

$$\lim_{T\to 0+} \chi_{k=\pi} = -(6y)^{-1}. \tag{5.12b}$$

Therefore, the dominant short-range magnetic order at $T=0+$ is ferromagnetic or antiferromagnetic (depending on the sign of y) for the uniform chain. For the dimerized alternating ($y_1>0, y_2<0$) chain, (5.8) is singular at $T=0$ only for $k=\pi/2$. $\chi_{k=\pi/2}$ then reads

$$\lim_{T\to 0+} \chi_{k=\pi/2} = \tfrac{2}{3}\beta^2 y_1 y_2/(y_2 - y_1), \tag{5.13}$$

for ($y_1>0, y_2<0$). Therefore, the dominant short-range magnetic order for the dimerized alternating chain is of period 4. As a result of the magnetoelastic coupling, the lattice distortion at $T>0$ has to produce a different long-range magnetic order for the 1D spin chain at $T=0$.

For a nonalternating chain (y_1 and y_2 of the same sign) χ_k is singular at $T=0$ only for $k=0$ ($k=\pi$) when $y_1<0$ ($y_2>0$). However, at $T=0$, we have seen in Sec. III that the dimerized chain is always alternating. Thus the first-order dimerization transition at $g=\pm(1-A)/2$ for $T=0$ is accompanied by a magnetic transition at the same value of g.

At finite T the dimerized state is not necessarily alternating, as shown in Figs. 7(a) and 8(a) when the uniform state bifurcates continuously to a dimerized nonalternating state. We have to get deeper into the dimerized region to obtain the alternating ground state. Some typical finite-T results for χ_k are shown in Figs. 7(b), 8(b), and 9(b). The results were obtained from the numerical evaluation of (5.8) with the (y_1,y_2) solutions of Figs. 7(a), 8(a), and 9(a). The immediate increase of $\chi_{k=\pi/2}$ (in comparison with other k values) at the phase transition is quite clear. As g goes to zero, $k=\pi/2$ is definitely the wave vector for which the magnetic susceptibility has the largest value. This has been checked with other k values not shown in Figs. 7, 8, and 9. Therefore, from these figures, it becomes clear that the dominant short-range magnetic order is of period 4 in the dimerized phase. When the transition is continuous, one must go deeper in the dimerized phase in order that the maximum of the magnetic susceptibility be located at $k=\pi/2$. As expected, the maximum of χ_k is at $k=\pi$ in the uniform state when $g>0$ since then the exchange integrals y are antiferromagnetic. Note that $\chi_{k=\pi} = \chi_{k=0}$ at $g=0$ (i.e., when $y_1 = -y_2$).

VI. CONCLUSION

We have shown that a three-dimensional lattice structure of one-dimensional classical spin chains can distort itself in the presence of a magnetoelastic coupling. In contrast with the quantum spin Peierls problem,[8,11] a positive second-neighbor elastic interaction is needed to have a dimerized ground state in a translationally invariant Hamiltonian with first-neighbor spin-exchange interactions. The action of 1D spin chains on the lattice structure is twofold. First, it screens the first-neighbor elastic interactions; and second, it renormalizes the pressure term

for nonzero values of J_0. Our calculations were performed at constant pressure. This approach has enabled us to predict that a dimerized phase can be reached by applying pressure to the appropriate magnetic material.

Moreover we have shown, by a calculation of the wave-number-dependent magnetic susceptibility, that the dominant short-range magnetic order in the dimerized phase is of period 4. This short-range order becomes a long-range order at $T=0$. Therefore, the lattice distortion produced by the magnetoelastic coupling has strongly affected the magnetic properties.

Finally, let us stress that, in view of the work of Janssen and Tjon,[16] incommensurate ground states should occur in this magnetoelastic problem if the bare lattice has third-neighbor elastic interactions, their quartic double-well first-neighbor term being replaced by $W(x)$. Again, the pressure term that naturally arises in this magnetoelastic problem could not create by itself any instability at another wave vector but would modify the equilibrium states (by a $q=0$ component) and change the phase boundaries.

ACKNOWLEDGMENTS

This work was supported by the Natural Sciences and Engineering Research Council of Canada, the Fonds pour la Formation de Chercheurs à l'aide à la Recherce du Québec and the Groupe de Recherche sur les Semiconducteurs et les Diélectriques.

APPENDIX A

In this appendix we show how to calculate the location of the tricritical point by its temperature dependence as a function of A. Recall that at a tricritical point, a second-order transition becomes first order. Therefore, the solution $(y_1, y_2=y_1+\epsilon)$ does not fulfill the stability conditions (3.6) as ϵ goes to zero when the transition becomes first order. To find the conditions under which this happens, we use the following expansion for small positive δ:

$$L(y)=L(x)+\delta L'(x)+\tfrac{1}{2}\delta^2 L''(x)+6^{-1}\delta^3 L'''(x)+\cdots , \tag{A1}$$

and rewrite (3.3) as

$$L(y)=L(x)+\tau\delta , \tag{A2}$$

where $x=\beta y_1$ and $y=\beta y_2=x+\delta$. Then, we can write

$$\tau=L'(x)+\tfrac{1}{2}\delta L''(x)+6^{-1}\delta^2 L'''(x)+\cdots . \tag{A3}$$

Therefore, the stability condition (3.6b), to first order in δ, can be written as

$$(1-A)L'(x)+\tfrac{1}{2}(1+A)\delta L''(x)>0 , \tag{A4}$$

which is always satisfied for $\delta\to 0$ and $A<1$.

Using (A1), (A2), and (A3), the stability condition (3.6a), to second order in δ, can be written as

$$\delta^2[3^{-1}(1-A)L'(x)L'''(x)+AL''(x)^2]<0 . \tag{A5}$$

Therefore, for a given A, the temperature τ_T of the tricritical point is given by

$$\tau_T=L'(x) , \tag{A6}$$

with x the solution of

$$3^{-1}(1-A)L'(x)L'''(x)+AL''(x)^2=0 . \tag{A7}$$

The numerical solutions of (A7) with τ_T given by (A6) are plotted in Fig. 4.

APPENDIX B

We consider the following classical Heisenberg Hamiltonian for an arbitrary collection of exchange integrals y_j:

$$H=\sum_{j=1}^{N-1} y_j \mathbf{S}_j\cdot\mathbf{S}_{j+1} \tag{B1}$$

and want to calculate the correlation function

$$\langle S_j^z S_{j+n}^z\rangle = Z^{-1}\int \frac{d\Omega_1}{4\pi}\cdots\frac{d\Omega_N}{4\pi} S_j^z S_{j+n}^z \exp(-\beta H) , \tag{B2}$$

where Z is the partition function for the Hamiltonian (B1):

$$Z=\prod_{l=1}^{N-1} z_l \tag{B3}$$

with

$$z_l=(\beta y_l)^{-1}\sinh(\beta y_l) . \tag{B4}$$

Each integral in (B2), for $l<j$ and $l>j+n$, gives z_l. Therefore, (B2) reduces to

$$\langle S_j^z S_{j+n}^z\rangle = \int \frac{d\Omega_j}{4\pi z_j}\cdots\frac{d\Omega_{j+n}}{4\pi z_{j+n}} S_j^z S_{j+n}^z \times\exp\left[-\beta\sum_{l=j}^{j+n-1} y_l \mathbf{S}_l\cdot\mathbf{S}_{l+1}\right] . \tag{B5}$$

By the spherical harmonics addition theorem,[17] we have

$$\exp(-\beta y_j \mathbf{S}_j\cdot\mathbf{S}_{j+1})=\sum_{l,m}\lambda_{lm}(y_j)Y_{lm}(\theta_j,\phi_j) \times Y_{lm}^*(\theta_{j+1},\phi_{j+1}) , \tag{B6}$$

with the eigenvalues $\lambda_{lm}(y_j)$ given by

$$\lambda_{lm}(y_j)=2\pi(-1)^m\int_{-1}^{+1} dx P_l(x)\exp[-\beta y_j x] , \tag{B7}$$

where $P_l(x)$ are the Legendre polynomials. Since $S_j^z=\cos(\theta_j)=(4\pi/3)^{1/2}Y_{10}(\theta_j,\phi_j)$, the first integral in (B5):

$$I=\int\frac{d\Omega_{j+n}}{4\pi}\cos(\theta_{j+n}) \times\exp(-\beta y_{j+n-1}\mathbf{S}_{j+n-1}\cdot\mathbf{S}_{j+n}) , \tag{B8}$$

by (B6), (B7), and the orthonormalization of the spherical harmonics Y_{lm}, becomes:

$$I=(12\pi)^{-1/2}\lambda_{10}(y_{j+n-1})Y_{10}(\theta_{j+n-1},\phi_{j+n-1})\ . \tag{B9}$$

Therefore, all the integrals for $l>j$ in (B5) are the same and the final result is easily obtained,

$$\langle S_j^z S_{j+n}^z\rangle=3^{-1}\prod_{l=j}^{j+n-1}[\lambda_{10}(y_l)/(4\pi z_l)] \tag{B10}$$

which, by (B4) and (B7), becomes

$$\langle S_j^z S_{j+n}^z\rangle=3^{-1}\prod_{l=j}^{j+n-1}L(-\beta y_l)\ . \tag{B11}$$

[1]J. Sak, Phys. Rev. B **10**, 3957 (1974).

[2]D. J. Bergman and B. I. Halperin, Phys. Rev. B **13**, 2145 (1976).

[3]M. A. de Moura, T. C. Lubensky, Y. Imry, and A. Aharony, Phys. Rev. B **13**, 2176 (1976).

[4]See Ref. 2 for an additional list of references.

[5]E. Pytte, Phys. Rev. B **10**, 2039 (1974).

[6]K. A. Penson, A. Holz, and K. H. Bennemann, Phys. Rev. B **13**, 433 (1976).

[7]K. A. Penson, A. Holz, and K. H. Bennemann, J. Chem. Phys. **65**, 5024 (1976).

[8]J. W. Bray, L. V. Interrante, I. S. Jacobs, and J. C. Bonner, *Extended Linear Chains Compounds,* edited by J. S. Miller (Plenum, New York, 1982), Vol. 3, pp. 353—415, and references therein.

[9]We should mention for the meticulous reader that, after the decomposition $x_{j+2}-x_j=v_{j+1}+v_j$, we have made the approximation $\sum_{j=2}^{N-1}v_j=\sum_{j=1}^{N-2}v_j=\sum_{j=1}^{N-1}v_j$ valid for $N\gg 1$.

[10]This can be easily shown by minimization of H with respect to the Fourier components of the bond variables v_j.

[11]G. Beni and P. Pincus, J. Chem. Phys. **57**, 3531 (1972).

[12]Here and henceforth, $\partial f_e/\partial_y$ is symbolized by $\partial_y f_e$.

[13]*Handbook of Mathematical Functions,* edited by M. Abramowitz and I. A. Stegun (Dover, New York, 1972).

[14]For example, for $J_0\sim -10$ (in units of $J_1^2/2K_1$), $A\sim 0.9$, and $J_1\sim 100$ K/Å, the applied pressure needed to get into the dimerized phase is estimated to be the order of 1 kbar for chains having cross sections of (10 Å)^2.

[15]M. E. Fisher, Am. J. Phys. **32**, 343 (1964).

[16]T. Janssen and J. A. Tjon, Phys. Rev. B **25**, 3767 (1982).

[17]E. Merzbacher, *Quantum Mechanics* (Wiley, New York, 1970).